Fabrication of chalcogenide microstructured optical preforms and fibers by additive manufacturing of chalcogenide glasses

Johann Troles, Julie Carcreff, François Cheviré, Ronan Lebullenger, Antoine Gautier, Radwan Chahal, Laurent Calvez, Catherine Boussard-Plédel, Laurent Brilland, Frédéric Charpentier, et al.

Fabrication of chalcogenide microstructured optical preforms and fibers by additive manufacturing of chalcogenide glasses

J. Troles[a], J. Carcreff[a], F. Cheviré[a,] R. Lebullenger[a], A. Gautier[a], R. Chahal[b], L. Calvez[a], C. Boussard[a,] L. Brilland[b] , F. Charpentier[c], H. Tariel[c], Y. Guimond[d], M. Roze[d], L. Szymczyk[a,d], G. Renversez [e]

[a] Univ Rennes, CNRS, ISCR-UMR 6226, F-35000 Rennes, France, [b] Selenoptics, 263 Avenue Gal Leclerc, 35042 Rennes, France, [c] Diafir, Parc Lorans, 26J, Avenue Chardonnet, 35 000 Rennes, France, [d] Umicore IR glass, ZA le Boulais, 35690 Acigné, France, [e] Aix–Marseille Univ, CNRS, Centrale Marseille, Institut Fresnel, UMR 7249, 13013 Marseille

ABSTRACT

In recent years, a growing interest has settled for optical materials and fibers for the mid infrared (mid-IR) region. This interest originates from societal needs for health and environment for instance, and also from demand for defence applications. Indeed, the mid-IR spectral region contains the atmospheric transparent windows (3-5 µm) and (8-12 µm) where thermal imaging (military and civilian) can take place. The elaboration of chalcogenide microstructured optical fibers (MOFs) permits to combine the mid infrared transmission of chalcogenide glasses up to 18 µm to the unique optical properties of MOFs thanks to the high degree of freedom in the design of their geometrical structure. In this context, additive manufacturing of glass materials appears as an attractive technique to achieve more elaborate designs that can hardly be obtain using more common methods such as the stack-and-draw or molding. Taking advantages of the specific physical properties of chalcogenide glasses such as low Tg and extrusion temperature, we have shown that chalcogenide preforms can be rapidly obtained by fused deposition modeling (FDM) using a customized RepRap-style 3D printed fed with chalcogenide glass rods. Such as-prepared preforms can be drawn into chalcogenide optical fibers. Those early-stage results open a new way for the elaboration of chalcogenide MOFs.

Keywords: Chalcogenide glasses, chalcogenide fibers, microstructured optical fibers, mid-infrared, 3D printing

1. INTRODUCTION

In recent years, the interest for optical materials and fibers operating in the mid infrared (mid-IR) region has grown tremendously. This interest originates from societal needs in the fields of health and environment for instance, and also from demand for defense applications. Indeed, the mid-IR spectral region contains the atmospheric transparent windows (3-5 µm) and (8-12 µm) where thermal imaging (military and civilian) can take place. Furthermore, the infrared window is well-suited for sensing (bio)-molecules, whose fingerprints are located at wavelengths between 2 and 15 µm. In this context, the development of mid-IR transparent materials and optical fibers is essential. Chalcogenide glasses are good candidates for the realization of new and innovative mid-IR systems. Thus, chalcogenide fibers have been utilized for versatile mid-IR fiber transmission [1, 2], supercontinuum generation [3, 4], and sensing [5-7]

An original way to obtain single-mode fibers is to design microstructured optical fibers (MOFs). Such fibers present unique optical properties thanks to the high degree of freedom in the design of their geometrical structure. Since the primary works on silica MOFs, this new class of fibers has attracted much interest in the optical fiber community[8, 9]. Different methods for the realization of chalcogenide preforms and microstructured fibers have been reported, such as the stack and draw method [10], drilling method [11, 12], extrusion processes [13, 14] and molding method [15].

In this context, we have investigated an alternative way for fabricating microstructured preforms by using an original 3D printing process. By using this additive manufacturing method, preforms with complex designs can be fabricated in a single step within a couple of hours, with a high degree of repeatability and precision of the geometry. The cost of

fabrication can be reduced as well, as compared to traditional techniques. In this study, the optical attenuation of the printed fiber has been compared to the one of a chalcogenide fiber drawn from a standard melt-quenched preform. Finally, the fabrication of a holey chalcogenide preforms is reported. A holey fiber has been drawn from the preform, and transmission of infrared light has been demonstrated.

2. THE CHOSEN CHALCOGENIDE GLASS: $TE_{20}AS_{30}SE_{50}$

2.1 Thermal properties

Calorimetric measurements were carried out with a differential scanning calorimeter (DSC). The glass transition temperature (Tg) was determined by heating 10 mg of a $Te_{20}As_{30}Se_{50}$ (TAS) sample in a hermetic aluminum pan at 10°C/min rate. Tg was measured at around 137 °C, as shown in figure 1. In addition, no crystallization peak has been observed up to 280 °C, which demonstrates the stability of the glass against crystallization.

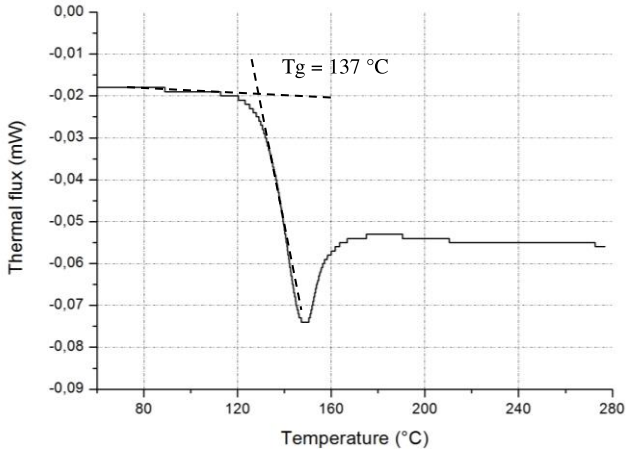

Figure 1. DSC Curve of the $Te_{20}As_{30}Se_{50}$ chalcogenide.

Viscosity measurements have been carried out by means of a parallel-plates experimental set-up. The lower viscosity than can be measured with this set-up is 10^4 Pa.s. The results are displayed in figure 2. By extrapolating with VFT equation the curve, a range of viscosity of 10-10^3 Pa.s can be estimated between 260 °C and 300 °C, which correspond to the conventional viscosities and temperatures used for standard thermal 3D printing of polymers [16]. As a result, one can assume that the additive manufacturing method can be implemented with TAS glass.

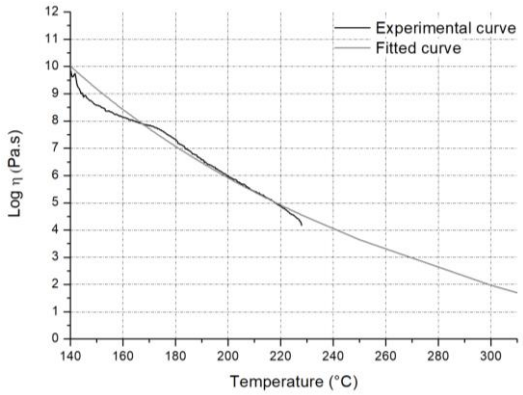

Figure 2. Viscosity curve of the Te20As30Se50 glass.

2.2 Optical properties

The main goal of this study is to explore a new way for the elaboration of chalcogenide MOFs, and more particularly for fabricating hollow-core fibers. Preliminary modelling works have been carried out in order to define the optimized design of the future fiber. For defining the best fiber geometry, optical properties of TAS glass, such as the refractive index and fiber attenuation, have to be considered.

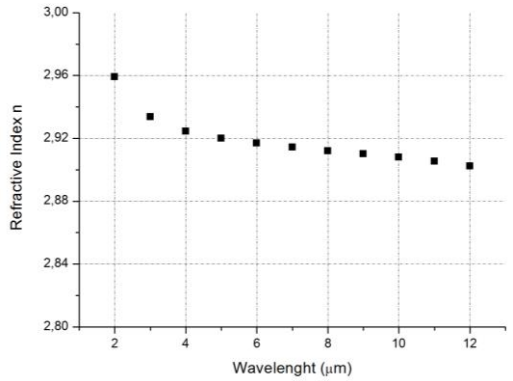

Figure 3. Refractive indices of the $Te_{20}As_{30}Se_{50}$ glass in the mid-IR.

Figure 3 presents the values of TAS glass refractive index as a function of wavelength. The refractive index varies from 2.96 (at 2 µm) to 2.90 (at 12 µm) [17]. The typical attenuation curve of a high purity TAS glass is presented in figure 4. The optical losses are less than 3 dB/m between 3 and 10 µm and less than 100 dB/m between 1 and 17 µm. Thanks to preliminary numerical modelling, we can expect an attenuation less than 10 dB/km at 10 µm in a TAS hollow core fiber.

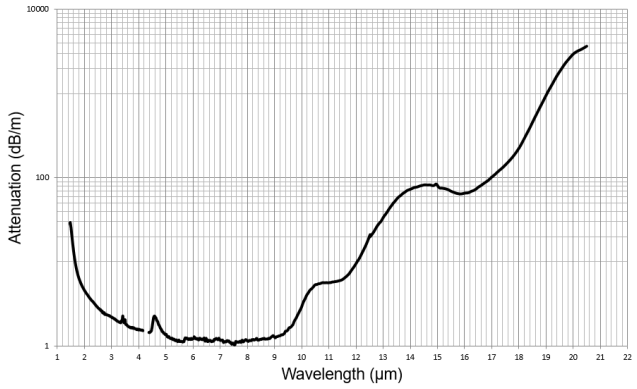

Figure 4. Optical Attenuation of a $Te_{20}As_{30}Se_{50}$ fiber.

3. CHALCOGENIDE GLASSES 3D PRINTING PROCESS

3.1 Homemade 3D printer

The principles of 3D printing can be found in Ref. [18]. In this study, the 3D-printing set-up is based on a customized commercial RepRap-style 3D printer (Anet A8) upgraded for soft glasses (Fig. 5). Especially, the feeding mechanism is customized for brittle materials. This mechanism is supplied with 400-mm long TAS rods with 1.75 to 3-mm diameters, produced by the fiber-drawing method. An extruder drives the raw material filament to a nozzle, heated well above Tg. The printer head moves in the X and Z directions and the bed plate in Y direction while depositing the TAS glass as a thin layer on the pan. The nozzle can control the diameter of the extruded filament from 250 µm to 400 µm.

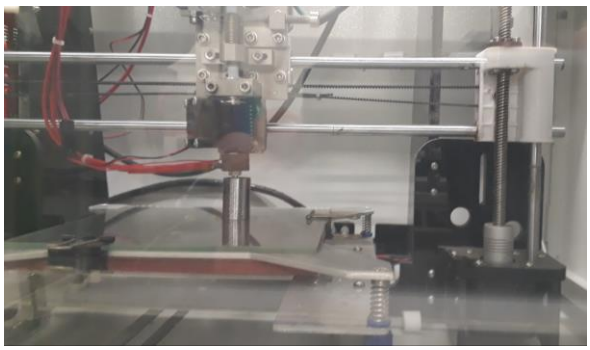

Figure 5. Photography of the 3D printer used for printing the chalcogenide glass.

The printer head, made in copper, can reach an extrusion temperature of 400 °C. As shown in figure 2, TAS glass reaches a suitable viscosity when the temperature is above 250 °C. In consequence, the temperature of the printer head and the nozzle was fixed at 300 °C. The size of the nozzle, and consequently, the thickness of the printed lines was about 400 µm. The TAS glass was deposited on a sodalime glass bed plate heated around 140 °C, which ensures a good adherence of the printed sample. The printer movements were controlled by using G-code programs especially computed for driving displacements compatible with TAS glass.

3.2 Characterizations of the 3D printed glasses and fibers

Firstly, TAS glass bulk pellets of 5 mm height and 10 mm diameter were printed and polished before being analyzed to compare the physical properties of the initial glass to those of the printed glass. The composition of the pellet was determined by energy dispersive spectroscopy (EDS). The results are shown in Table 1. The comparison with the initial composition of the glass indicates that there is no change in the chemical composition during the printing process. The glass transition temperature (T_g), thermal expansion coefficient (α), and density of the printed TAS glass were also compared to a standard TAS glass (see Table 1). Considering the experimental error inherent to DSC measurements (DSC Q20 Thermal Analysis), the T_g of the printed glass and the initial glass are similar. In addition, no crystallization peak was observed in the DSC measurement of the printed glass (not shown). The thermal coefficient measurements were carried out on a thermomechanical analyzer (TA Instrument, TMA 2940) with a heating ramp of 2 °C·min^{-1}. The coefficient is 22.82·10^{-6} K^{-1} for a classic glass and 22.62·10^{-6} K^{-1} for a printed glass, respectively. Considering the measurement error, both glasses have the same coefficient of expansion. The densities were measured by the Archimedes method. It is noticed that the density significantly decreases from 4.86 g·cm^{-3} for a quenched glass to 4.81 g·cm^{-3} for a printed glass, meaning that the printed objects do not present the expected density of a bulk glass. To ensure that the glass did not crystallize during the additive manufacturing process, the initial and the printed TAS pellets were analyzed by X-ray diffraction (XRD). XRD diagrams were recorded at room temperature in the 10–80° 2θ range. It has been observed (not shown) that the XRD diagrams of the initial glass and the printed glass perfectly overlap and no additional diffraction peak is detected for the printed glass.

Table 1. Physical properties comparison of a melt/quenched TAS glass used as the initial glass and a printed TAS glass

	Initial TAS Glass	**Printed TAS Glass**
Composition from EDS analysis (%) (±1)	$Te_{20}As_{30}Se_{50}$	$Te_{21}As_{29}Se_{50}$
Tg (°C) (±2)	137	136
Coefficient of thermic expansion (10^{-6} K^{-1}) (± 1%)	22.82	22.62
Density (g.cm^{-3}) (± 0.02)	4.86	4.81

After pellets, two cylinders (or preforms) with an outer diameter of 8 mm were printed. One of the cylinders was obtained from an unpurified TAS glass rod while the second one was obtained from a purified glass rod. These preforms were prepared in order to be drawn and optically characterized with the aim to compare the optical losses between initial glass fibers and printed glass fibers depending on the quality of the initial glass.

Each preform was stretched on a drawing tower specifically designed for low Tg glasses. Several meters of fibers with approximately a 400 µm diameter were obtained and optically characterized using the FTIR and a MCT (alloy of mercury, cadmium and tellurium) detector. Attenuation measurements were performed in order to compare the optical transmission of the initial glass fibers and the "printed" fibers. The results are shown in Figure 6. A significant increase in optical losses is observed for the "printed" fibers. Thus, when the minimum attenuation of the initial unpurified glass is less than 10 dB/m, and less than 1 dB/m for the purified glass, the minimum attenuation of the unpurified “printed” fiber is around 28 dB/m and around 18 dB/m for the purified "printed" fiber.

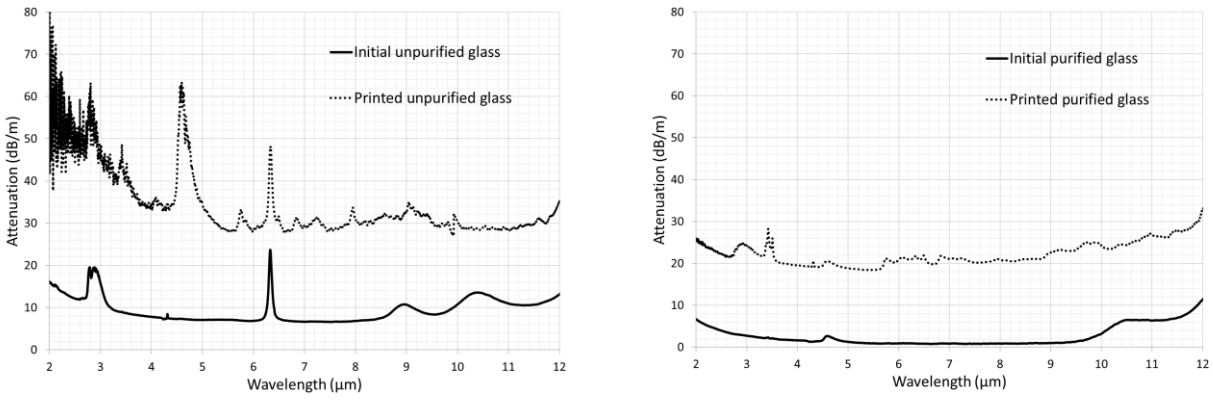

(a) (b)

Figure 6. Comparison of Attenuation spectra of initial and printed glasses: (a) with an unpurified initial glass (b) with purified initial glass

3.3 3D printing of microstructured preforms and fibers

Finally, additive manufacturing was applied to the printing of fiber preforms as shown in Fig 7. As example, preforms with a clad and 6 or 8 capillaries could be printed. The 3D printing method permit also to print original designs as examples with semi-circles or triangles (see Fig. 7c and Fig. 7b).

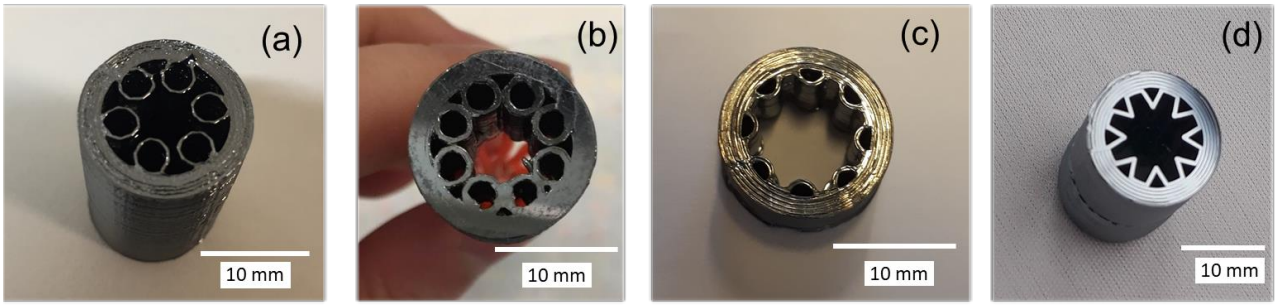

Figure 7. Printed preforms: (a) cross-section view of the chalcogenide printed 6 capillaries preform (b) cross-section view of the chalcogenide printed 8 capillaries preform (c) cross-section view of the chalcogenide printed 8 half-capillaries preform (c) cross section view of 8 triangles preform.

From the preform with 6 capillaries, a microstructured optical fiber could be drawn [19]. The printed preform was used to manufacture an anti-resonant hollow-core fiber by using a homemade drawing tower specifically designed for low-Tg glasses. The preform is placed in a narrow drawing furnace that can permit to draw short preforms. When the furnace

reaches the drawing temperature around 270° C, a glass drop appears and falls down under gravity forming a glass fiber which is then reeled on a spool in rotary motion. At the same time, the preform is moved down, feeding the drawing furnace. For a given feeding speed of the preform, the diameter of the fiber is controlled by the spool speed. A helium gas flow provides an inert atmosphere around the preform. Usually, during the drawing of MOFs, a differential pressure is applied in the core and in the different capillaries in order to control the geometry. However, for this proof of concept study, no differential pressure was applied. Consequently, the geometry of the capillaries has changed during drawing due to surface tension, more particularly the ratio between the inner and the outer diameter. Nevertheless, it has been demonstrated that a preform obtained by additive manufacturing can be drawn into a fiber in which the initial shape is globally maintained (see Fig. 3). Although the printed hollow core preform is only 3 cm long, only several meters of fibers have been obtained. The optical losses of the "printed fiber" were too high to perform cut back analysis, however, light transmission of a 20-cm long hollow-core fiber drawn from the printed preform has been obtained in the 2 -12 um Mid-IR window (Fig 8).

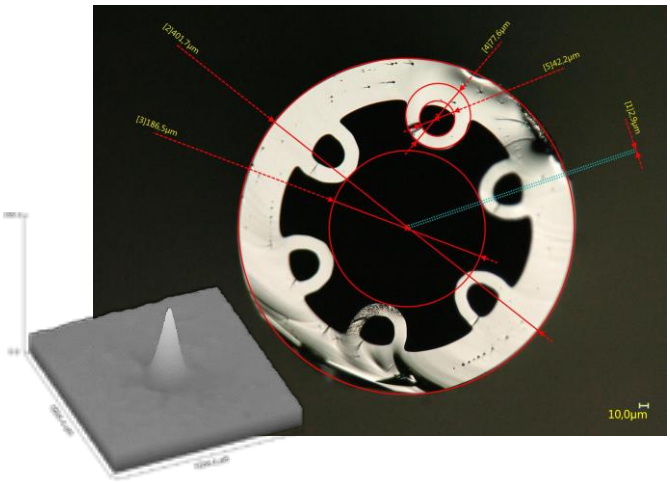

Figure 8. Chalcogenide hollow core fiber obtained from a printed preform (from Fig.6a), inset Mid-IR output profile recorder with a microbolometer camera in the [7-13 µm] range.

4. CONCLUSION

This work clearly demonstrates that 3D printing could be an innovative approach for elaborating microstructured fibers. Especially, it allows one to obtain new geometries that cannot be realized by any other methods such as stack and draw, extrusion or molding. This innovative 3D printing method opens the way to many applications involving chalcogenide fiber manufacturing, but also many other optical devices based on chalcogenide glasses, such as chalcogenide sensors for spectroscopy and medical diagnosis.

5. AKNOWLEGEMENT

This work was funded in part by the European Union through the European Regional Development Fund (ERDF), the Ministry of Higher Education and Research, the French region of Brittany, Rennes Métropole, the French defense innovation agency (AID), grant ANR ASTRID MIR-3D and by a grant overseen by the French National Research Agency (ANR) as part of the "France 2030" Program, the Equipex ADD4P .

REFERENCES

[1] G. Tao, H. Ebendorff-Heidepriem, A. M. Stolyarov et al., "Infrared fibers", Advances in Optics and Photonics, vol. 7(2). 379-458 (2015).

[2] S. Maurugeon, C. Boussard-Pledel, J. Troles et al., "Telluride Glass Step Index Fiber for the far Infrared, Journal of Lightwave Technology", vol. 28(23). 3358-3363, (2010).

[3] S. X. Dai, Y. Y. Wang, X. F. Peng et al., "A Review of Mid-Infrared Supercontinuum Generation in Chalcogenide Glass Fibers", Applied Sciences-Basel, vol. 8(5). 28, (2018).

[4] S. Venck, F. St-Hilaire, L. Brilland et al., "2-10 mu m Mid-Infrared Fiber-Based Supercontinuum Laser Source: Experiment and Simulation", Laser & Photonics Reviews, vol. 14(6). (2020).

[5] M. L. Brandily, V. Monbet, B. Bureau et al., "Identification of foodborne pathogens within food matrices by IR spectroscopy", Sensors and Actuators B: Chemical, vol. 160(1), 202-206, (2011).

[6] P. Toupin, L. Brilland, C. Boussard-Pledel et al., "Comparison between chalcogenide glass single index and microstructured exposed-core fibers for chemical sensing", Journal of Non-Crystalline Solids, vol. 377. 217-219, (2013).

[7] A. B. Seddon, B. Napier, I. Lindsay et al. "Prospective on using fibre mid-infrared supercontinuum laser sources for in vivo spectral discrimination of disease, Analyst, vol. 143(24). 5874-5887, (2018).

[8] T. A. Birks, P. J. Roberts, P. S. J. Russell et al., "Full 2-D photonic bandgaps in silica/air structures", Electronics Letters, vol. 31(22). 1941-1943, (1995).

[9] P. Russell: Photonic Crystal Fibers, Science, vol. 299;5605 358, (2003).

[10] F. Desevedavy, G. Renversez, J. Troles et al. "Chalcogenide glass hollow core photonic crystal fibers, Optical Materials", vol. 32(11). 1532-1539, (2010).

[11] P. Zhang, J. Zhang, P. Yang et al.: "Fabrication of chalcogenide glass photonic crystal fibers with mechanical drilling", Optical Fiber Technology, vol. 26, Part B. 176-179, (2015).

[12] M. El-Amraoui, G. Gadret, J. C. Jules et al., "Microstructured chalcogenide optical fibers from As2S3 glass: towards new IR broadband sources", Opt. Express, vol. 18(25), 26655-26665, (2010).

[13] R. R. Gattass, D. Rhonehouse, D. Gibson et al., "Infrared glass-based negative-curvature anti-resonant fibers fabricated through extrusion", Optics Express, vol. 24(22), 25697-25703, (2016).

[14] Z. G. Xue, S. Liu, Z. M. Zhao et al.: "Infrared Suspended-Core Fiber Fabrication Based on Stacked Chalcogenide Glass Extrusion", Journal of Lightwave Technology, vol. 36(12), 2416-2421, (2018).

[15] P. Toupin, L. Brilland, J. Trolès et al., "Small core Ge-As-Se microstructured optical fiber with single-mode propagation and low optical losses", Optical Materials Express, vol. 2(10), 1359-1366, (2012).

[16] Y. I. Yoon, K. Park, S. J. Lee et al.: "Fabrication of Microfibrous and Nano-/Microfibrous Scaffolds: Melt and Hybrid Electrospinning and Surface Modification of Poly(L-lactic acid) with Plasticizer", BioMed research international, vol. 2013 309048, (2013).

[17] P. Houizot, C. Boussard-Pledel, A. J. Faber et al., "Infrared single mode chalcogenide glass fiber for space", Optics Express, vol. 15(19), 12529-12538, (2007).

[18] T. D. Ngo, A. Kashani, G. Imbalzano et al., "Additive manufacturing (3D printing): A review of materials, methods, applications and challenges", Composites Part B: Engineering V 143. 1-300, (2018).

[19] J. Carcreff, P. Masselin, C. Boussard-Pledel, P. Kulinski, J. Troles, and D. Le Coq, "Step-index fibre from metal halide chalcogenide glasses" Optical Materials Express 10, 2792-2804 (2020).